Received: 15 June 2019 | Revised: 3 October 2019 | Accepted: 4 October 2019

DOI: 10.1002/ardp.201900174

DPhG ARCH PHARM Archiv der Pharmazie

FULL PAPER

Bioassay of ferulic acid derivatives as influenza neuraminidase inhibitors

Man-Ying Cui[1] | Meng-Wu Xiao[1] | Lv-Jie Xu[2] | Yun Chen[1] | Ai-Lin Liu[2] | Jiao Ye[1] | Ai-Xi Hu[1]

[1]College of Chemistry and Chemical Engineering, Hunan University, Changsha, China

[2]Institute of Materia Medica, Chinese Academy of Medical Sciences and Peking Union Medical College, Beijing, China

Correspondence
Jiao Ye and Aixi Hu, College of Chemistry and Chemical Engineering, Hunan University, 410082 Changsha, China.
Email: yejiao@hnu.edu.cn, (J. Y.) and axhu@hnu.edu.cn (A. H.)

Funding information
Hunan Provincial Natural Science Foundation of China, Grant/Award Number: 2019JJ40030

Abstract

Four series of ferulic acid derivatives were designed, synthesized, and evaluated for their neuraminidase (NA) inhibitory activities against influenza virus H1N1 in vitro. The pharmacological results showed that the majority of the target compounds exhibited moderate influenza NA inhibitory activity, which was also better than that of ferulic acid. The two most potent compounds were **1m** and **4a** with IC_{50} values of 12.77 ± 0.47 and 12.96 ± 1.34 μg/ml, respectively. On the basis of the biological results, a preliminary structure–activity relationship (SAR) was derived and discussed. Besides, molecular docking was performed to study the possible interactions of compounds **1p**, **2d**, **3b**, and **4a** with the active site of NA. It was found that the 4-OH-3-OMe group and the amide group (CON) of ferulic acid amide derivatives were two key pharmacophores for NA inhibitory activity. It is meaningful to further modify the natural product ferulic acid to improve its influenza NA inhibitory activity.

KEYWORDS

ferulic acid derivatives, molecular docking, neuraminidase inhibitors

1 | INTRODUCTION

Influenza is an acute viral infectious disease of the respiratory tract. According to statistics from the World Health Organization, seasonal influenza could cause 2–5 million infections and 250,000–500,000 deaths each year worldwide.[1,2] With the long-term research on the influenza virus, it was found that there are two main glycoproteins—hemagglutinin (HA) and neuraminidase (NA) on the surface of the virus, which are responsible for the invasion of virus and the release of offspring virus, respectively.[3,4] Moreover, further research indicated that over 10 amino acid residues of NA's active site are highly conserved.[5,6] Hence, compared with other targets, NA is an attractive target for anti-influenza research. However, although there are two marketed NA inhibitors, oseltamivir and zanamivir, the drug resistance caused by the high mutability of the influenza virus has become increasingly severe.[7–9] As to the drug resistance of viruses, nonclassical influenza NA inhibitor may be a new research direction. In recent years, some nonclassical influenza NA inhibitors have been discovered possessing effective NA inhibitory activity such as the natural product licochalcone,[10] resveratrol,[11] kaempferol,[12] and so on. So it is a good way to discover new NA inhibitors from natural products.

Ferulic acid, a very common natural product, has a wide range of pharmacological activities, such as antioxidant, anti-inflammatory, antithrombotic, anticancer, and so on.[13] In 2016, it was reported that ferulic acid had moderate NA inhibitory activity with an IC_{50} value of 27.16 μg/ml.[14] However, to date, there are no follow-up reports about ferulic acid derivatives as influenza NA inhibitors. In 2017, Enkhtaivan et al.[15] found that piperazine structural fragment can significantly enhance the NA inhibitory activity of the natural product berberine (Figure 1a). In our previous research, it was found that the compounds containing piperazine fragments tend to exhibit moderate NA inhibitory activity with an IC_{50} value of 20.03 μg/ml[16] (Figure 1b). Besides, we found that thiazolamide fragments also can act as NA inhibitory active fragments in many NA inhibitors[17,18] (Figure 1c,d). On the basis of the above research, we took phenylacrylic acid as the basic fragment to condense with active piperazine fragments to design and synthesize the target

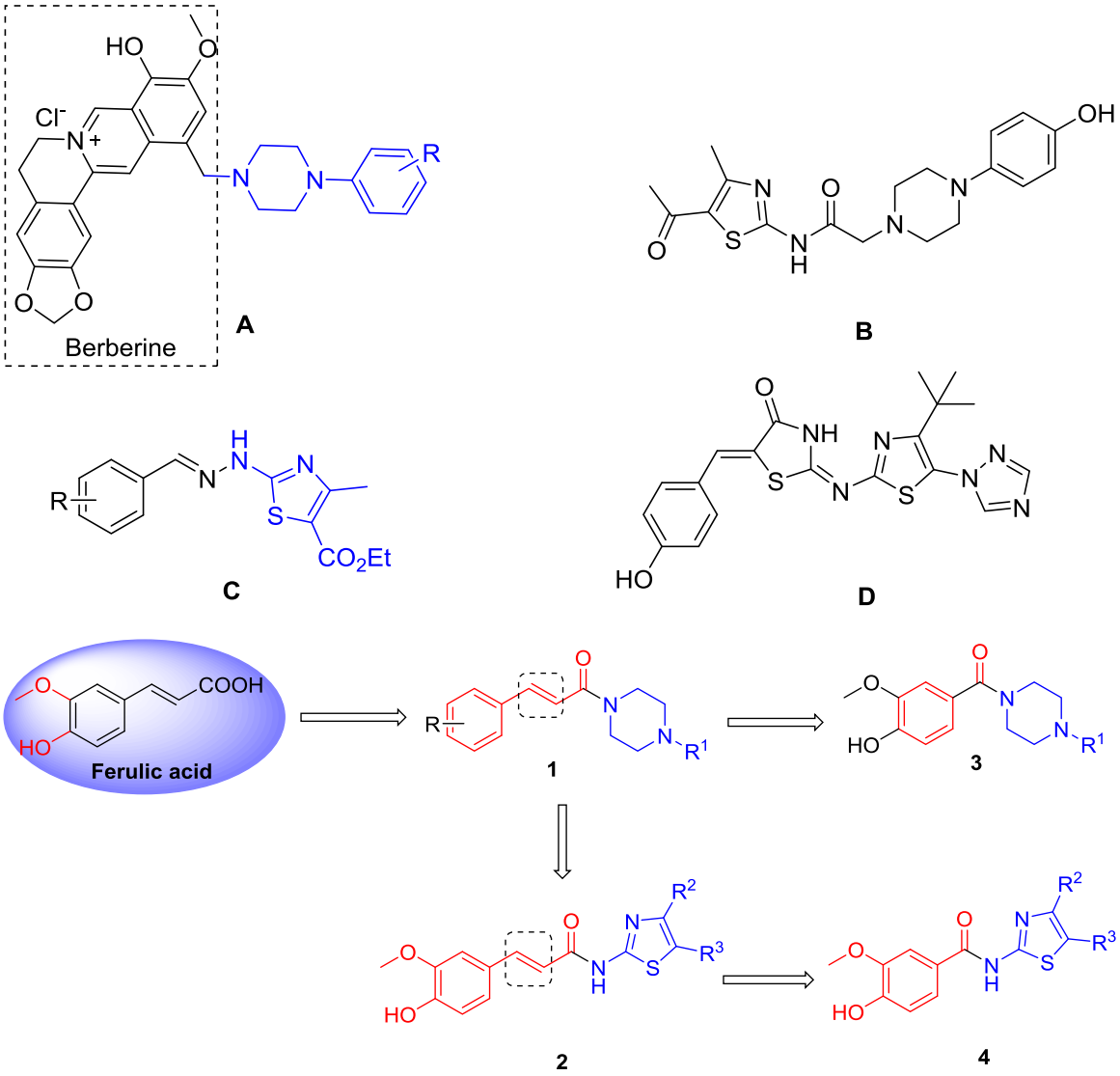

FIGURE 1 Design of the target compounds

compound **1**. According to the preliminary activity results, it can be found that 4-OH-3-OMe groups on the benzene ring of ferulic acid are the key pharmacophores on NA inhibitory activity. So keeping active pharmacophore (R = 4-OH-3-OMe), we spliced the ferulic acid with 2-aminothiazolyl fragments to design the target compound **2**. To further optimize the target compounds **1** and **2** with better activity and have a discussion on the structure–activity relationship, we removed the carbon–carbon double bond in target compounds **1** and **2** to design the target compounds **3** and **4** (Figure 1).

2 | RESULTS AND DISCUSSION

2.1 | Chemistry

The synthetic pathways of ferulic acid derivatives are shown in Scheme 1. The key intermediate substituted cinnamic acids **6** were synthesized as reported in the literature.[19] Substituted cinnamic acid **6** and various piperazine derivatives **7** were condensed using EDCI/HOBt as the condensing agent to afford cinnamamide derivatives **1a–q** with good yields. Due to the poor reactivity of 2-aminothiazolyl, it needed to be raised to 115°C to synthesize compounds **2a–f** using EDCI/HOBt as the condensing agent with moderate yields. Vanillic acid **6i** and piperazine derivatives **7** were condensed to prepare analogues **3a–c**, using the same method as in the synthesis of compound **1** with yields of 53.6%, 88.7%, and 64.3%, respectively. Vanillic acid was subjected to acetylation, condensation, and hydrolysis in turn to obtain the target compounds **4a–c**. In addition, the Boc-amine of compound **1q** was deprotected under the action of hydrogen chloride gas in ethyl acetate to obtain compound **1r**. Compound **1f** was hydrolyzed by LiOH aqueous solution to afford the compound **1s**. Compound **2h** was synthesized in the same way as in the synthesis of compound **1s**. Compound **2e** was condensed with methoxyammonium chloride to afford the compound **2g**. All the target compounds were characterized by NMR spectroscopy.

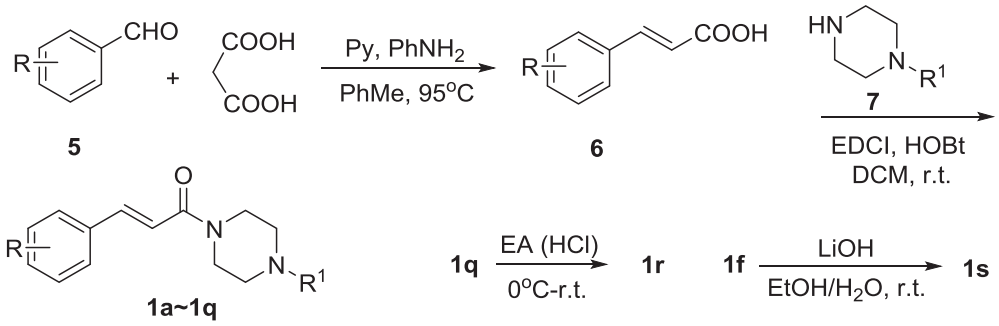

1a-1i: R^1 = 4-OHC_6H_4; **1a**: R = 3-OH; **1b**: R = 4-OH; **1c**: R = 3,4-$(OH)_2$; **1d**: R = 4-OMe; **1e**: R = 4-NO_2; **1f**: R = 4-CO_2Me; **1g**: R = 3-OH-4-OMe; **1h**: R = 3,5-$(OMe)_2$-4-OH; **1i**: R = 4-OH-3-OMe; **1j-1r**: R = 4-OH-3-OMe; **1j**: R^1 = 2-$OMeC_6H_4$; **1k**: R^1 = 4-ClC_6H_4; **1l**: R^1 = Ph; **1m**: R^1 = CH_3; **1n**: R^1 = C_2H_5; **1o**: R^1 = $COCH_3$; **1p**: R^1 = CO_2Et; **1q**: R^1 = Boc; **1r**: R^1 = H·HCl; **1s**: R = 4-COOH, R^1 = 4-OHC_6H_4

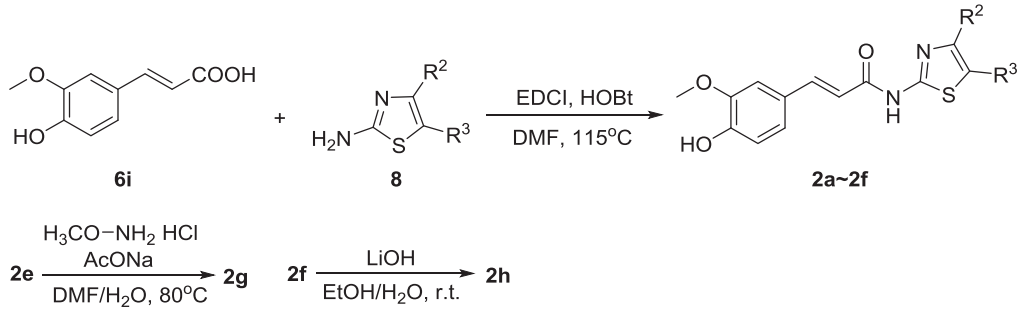

2a: R^2 = *t*-Bu, R^3 = NO_2; **2b**: R^2 = *t*-Bu, R^3 = imidazolyl; **2c**: R^2 = *t*-Bu, R^3 = 1,2,4- triazolyl; **2d**: R^2 = Me, R^3 = CO_2Et; **2e**: R^2 = Me, R^3 = $COCH_3$; **2f**: R^2 = CH_2CO_2Et, R^3 = H; **2g**: R^2 = Me, R^3 = C $(NOCH_3)CH_3$; **2h**: R^2 = CH_2COOH, R^3 = H

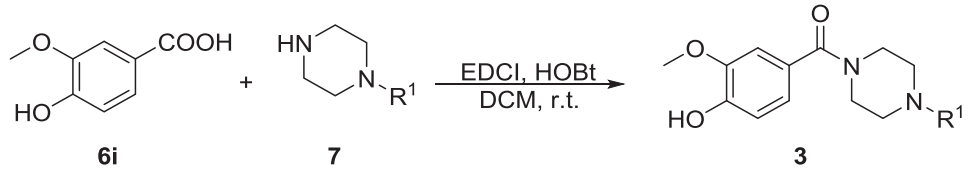

3a: R^1 = Boc; **3b**: R^1 = CO_2Et; **3c**: R^1 = 4-OHC_6H_4

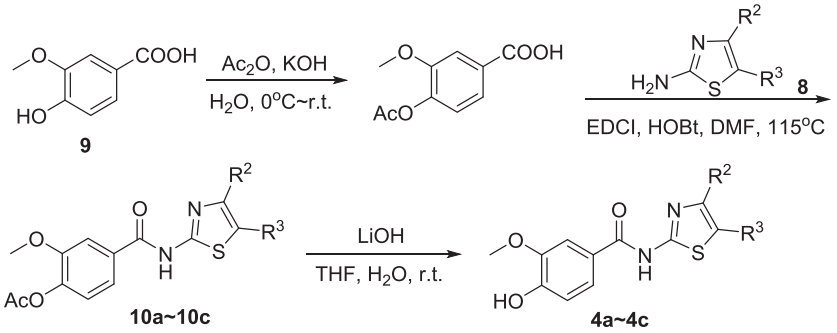

4a: R^2 = Me, R^3 = CO_2Et; **4b**: R^2 = Me, R^3 = $COCH_3$; **4c**: R^2 = *t*-Bu, R^3 = imidazolyl;

SCHEME 1 Synthesis of the target compounds

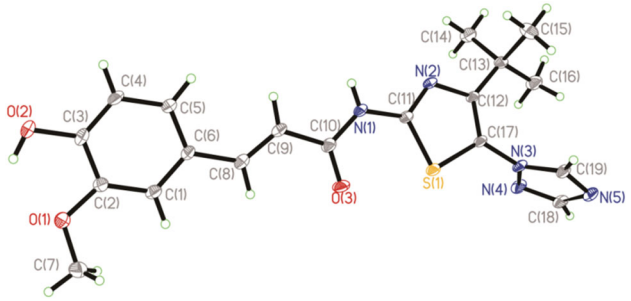

FIGURE 2 X-ray crystal structure of compound **2c**

2.2 | Crystal structure

Compound **2c** was determined by single-crystal X-ray diffraction. Yellow crystal of compound **2c** was obtained by slow evaporation of ethanol and water solution at room temperature. The crystal structure of compound **2c** is shown in Figure 2. The space group $P2_1/c$ is as follows: a = 10.43 (3), b = 10.642 (14), c = 17.35 (4) Å, α = 90°, β = 90.12 (3)°, γ = 90°, Z = 4, V = 1,926 (7) Å^3, F(000) = 840, Mr = 399.47, Dx = 1.377 mg m^{-3}, μ = 0.20 mm^{-1}, T = 273 K, Mo Kα radiation, λ = 0.71073 Å. As depicted in Figure 2, the CH═CH double bond (C8═C9) of acrylamide is present in the form of geometric *E* isomer, which is consistent with the coupling constant (J = 15.6 Hz) of *E* double bond in the ^{1}H NMR spectrum. The dihedral angle between phenyl plane and thiazole ring is 18.10°; the dihedral angle between the thiazole ring and the 1,2,4-triazole ring is 83.90°. As shown in Figure 3, the crystal structure is stabilized via intermolecular hydrogen bond interaction (N1-HA1...N5). The hydrogen bond length and angle are 2.956 Å and 164.74°, respectively. The additional crystal structure and experimental data are available from Supporting Information S1 and the Cambridge Crystallographic Data Centre as CCDC 1890182.

2.3 | In vitro inhibitory activity on NA

Thirty-three target compounds were synthesized and evaluated for the NA inhibitory activity against influenza viral NA (H1N1) at the concentration of 40 μg/ml in vitro using oseltamivir as positive control. The results of four series of thiazolylhydrazone derivatives are summarized in Tables 1–4. Preliminary biological results showed that many compounds displayed moderate to good inhibitory activity against NA.

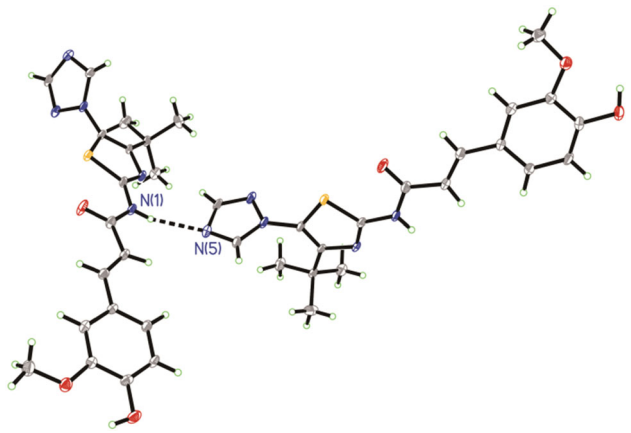

FIGURE 3 Hydrogen bond diagram of compound **2c**

As shown in Table 1, the majority of compound **1** had a moderate NA inhibitory activity. Especially, most of compounds **1i**–**r** with the 4-OH-3-OMe group on the phenyl ring tended to exhibit better NA inhibitory activity than compounds **1a**–**h**. Therefore, it can be speculated that 4-OH-3-OMe on the benzene ring played a decisive role on the inhibitory activity of NA and the 4-OH-3-OMe group was a critical pharmacophore.

Among compounds **1i**–**r** (R = 4-OH-3-OMe), compounds **1i**, **1m**, **1n**, **1o**, **1p**, and **1r** showed the better activity with IC_{50} values ranging from 10 to 20 μg/ml. Especially, compound **1m** (R = 4-OH-3-OMe, $R^1 = CH_3$) had the best activity with an IC_{50} value of 12.77 ± 0.47 μg/ml. The activity of compound **1j** (4-OH-3-OMe, $R^1 = 2\text{-}OMeC_6H_4$) and **1q** (R = 4-OH-3-OMe, R^1 = Boc) was relatively poor with IC_{50} values of 23.56 ± 0.52 and 24.52 ± 1.93 μg/ml. The inhibition rates of compound **1k** and **1l** were even less than 50% at the concentration of 40 μg/ml. The influence on activities of substituents R^1 on the piperazine ring is as follows: CH_3 > 4-OHC_6H_4 > H·HCl ≈ $COCH_3$ ≈ CO_2Et > C_2H_5 > 2-$OMeC_6H_4$ > Boc > Ph > 4-ClC_6H_4. On the basis of the above active order, it can be found that the activity of hydrophilic substituents on R^1 is better than that of hydrophobic substituents.

As shown in Table 2, most of compound **2** exhibited moderate NA inhibitory activity. The most potent one was compound **2g** (R^2 = Me, $R^3 = C(NOCH_3)CH_3$) with an IC_{50} value of 14.32 ± 0.06 μg/ml. The IC_{50} values of compounds **2b**–**e** ranged from 10 to 20 μg/ml. The activity of compound **2f** ($R^2 = CH_2CO_2Et$, R^3 = H) was relatively poor with an IC_{50} value of 24.64 ± 0.93 μg/ml. However, the hydrolyzed compound **2h** ($R^2 = CH_2COOH$, R^3 = H; IC_{50} = 18.47 ± 0.34 μg/ml) showed better activity than compound **2f**. The influence on the activities of substituent groups at 4-position and 5-position of the thiazole ring is as follows: 4-Me-5-$C(NOCH_3)CH_3$ > 4-Me-5-$COCH_3$ ≈ 4-Me-5-CO_2Et > 4-*t*-Bu-5-imidazolyl ≈ 4-*t*-Bu-5-1,2,4-triazolyl > 4-CH_2COOH > 4-CH_2CO_2Et-5-H > 4-*t*-Bu-5-NO_2. Preliminary structure–activity relationship shows that electron-withdrawing substituent (imidazolyl, 1,2,4-triazolyl, CO_2Et, $COCH_3$, $C(NOCH_3)CH_3$), which can form a conjugation with the thiazole ring can contribute to improvement of NA inhibitory activity. Besides, the increasing hydrophilicity of R^2 and R^3 groups can improve NA inhibitory activity.

To investigate the effect of the length of the carbon chain between the two rings on the inhibitory activity of NA, compounds **3** and **4** were designed, synthesized, and evaluated for NA inhibitory activity. The activity test results indicated that compound **3** possessed poor activities with an NA inhibition rate lower than 50% at the test concentration of 40 μg/ml (Table 3). Compound **4** had the equivalent activity with ferulic acid thiazolylamide derivatives **2** (Table 4). The compound **4a** (R = 4-OH-3-OMe, $R^1 = CH_3$) had better activity than others with an IC_{50} value of 12.96 ± 1.34 μg/ml. Comparing the activity, we can speculate that carbon–carbon double bonds play a key role in the activity of ferulic acid piperazine amide derivatives **1**. However, carbon–carbon double

TABLE 1 Inhibitory activity of compound **1** against neuraminidase in vitro

Comp 1	R	R^1	Inhibition rate (%)	IC_{50} (μg/ml)
1a	3-OH	4-OHC_6H_4	3.78	NA
1b	4-OH	4-OHC_6H_4	34.69	NA
1c	3,4-$(OH)_2$	4-OHC_6H_4	29.00	NA
1d	4-OMe	4-OHC_6H_4	2.53	NA
1e	4-NO_2	4-OHC_6H_4	4.39	NA
1f	4-CO_2Me	4-OHC_6H_4	7.03 ± 1.43	NA
1g	3-OH-4-OMe	4-OHC_6H_4	55.25 ± 5.79	33.94 ± 7.35
1h	4-OH-3,5- $(OMe)_2$	4-OHC_6H_4	38.01 ± 3.18	NA
1i	4-OH-3-OMe	4-OHC_6H_4	72.38 ± 0.50	19.06 ± 1.64
1j	4-OH-3-OMe	2-$OMeC_6H_4$	62.99 ± 1.08	23.56 ± 0.52
1k	4-OH-3-OMe	4-ClC_6H_4	29.60	NA
1l	4-OH-3-OMe	Ph	40.36	NA
1m	4-OH-3-OMe	CH_3	80.96 ± 1.70	12.77 ± 0.47
1n	4-OH-3-OMe	C_2H_5	75.25 ± 1.32	16.09 ± 0.96
1o	4-OH-3-OMe	$COCH_3$	76.23 ± 2.06	16.56 ± 0.59
1p	4-OH-3-OMe	CO_2Et	74.54 ± 0.25	18.36 ± 0.69
1q	4-OH-3-OMe	Boc	64.07 ± 1.7	24.52 ± 1.93
1r	4-OH-3-OMe	H·HCl	76.62 ± 0.84	16.21 ± 0.64
1s	4-COOH	4-OHC_6H_4	1.17	NA

bonds have almost no effect on the activity of ferulic acid thiazolylamide derivatives **2**. To sum up, the SAR of the ferulic acid derivatives is summarized in Figure 4.

2.4 | Docking analysis

To understand the interaction between ferulic acid derivatives and the NA active site, analogs **1p**, **2d**, **3b**, and **4a** containing ethoxycarbonyl group (CO_2Et) were respectively docked into the active sites of NA (H1N1, PDB entry: 3TI6) using LeDock (http://www.lephar.com/) with default parameters.[20,21] The results were analyzed and visualized using PyMOL (http://pymol.sourceforge.net/). LigPlot + v.2.1 was used to depict the two-dimensional (2D) interaction diagrams.[22]

TABLE 2 Inhibitory activity of compound **2** against neuraminidase in vitro

Comp 2	R^2	R^3	Inhibition rate (%)	IC_{50} (μg/ml)
2a	*t*-Bu	NO_2	45.29	NA
2b	*t*-Bu	imidazol-1-yl	72.2 ± 1.28	19.21 ± 1.13
2c	*t*-Bu	1,2,4-triazol-1-yl	69.34 ± 0.93	19.25 ± 0.14
2d	Me	CO_2Et	80.73 ± 1.07	15.93 ± 1.22
2e	Me	$COCH_3$	78.46 ± 1.19	14.38 ± 0.93
2f	CH_2CO_2Et	H	63.83 ± 0.73	24.64 ± 0.93
2g	Me	$C(NOCH_3)CH_3$	83.68 ± 1.09	14.32 ± 0.06
2h	CH_2COOH	H	75.06 ± 3.64	18.47 ± 0.34

According to the docking result in Figures 5a1 and 6a2, it could be found that the plane of the benzene ring of compound **1p** almost coincides with the plane of the six-membered ring of oseltamivir. There are eight hydrogen bonds formed between compound **1p** and the amino acid residues of NA. The stretching direction and angle of 4-OH-3-OMe on the benzene ring of compound **1p** are consistent with that of the acetamido group of oseltamivir. The 4-OH-3-OMe group on the benzene ring can strongly interact with residues of Arg152, Trp178 by two hydrogen bonds, which can explain the reason why the 4-OH-3-OMe group on the benzene ring has a dominant effect on activity. Besides, the stretching direction and angle of amide group (CON) of compound **1p** are accordant with the ester group of oseltamivir. Docking result demonstrates that the amide group (CON) of compound **1p** can form five hydrogen bonds with amino acid residues of Arg371, Try406, and Arg292, which contribute to the improvement of activity greatly. At last, the ester group (CO_2Et) of piperazine amide can also form a hydrogen bond with the amino acid residue of Asn294. However, as shown in Figures 5b1 and 6b2, compound **3b** cannot bind well to the NA cavity. There are just two hydrogen bonds with amino acid residues and the amide

TABLE 3 Inhibitory activity of compound **3** against neuraminidase in vitro

Comp 3	R^1	Inhibition rate (%)	IC_{50} (μg/ml)
3a	Boc	13.76	NA
3b	CO_2Et	17.39	NA
3c	4-OHPh	21.09	NA

TABLE 4 Inhibitory activity of compound **4** against neuraminidase in vitro

Comp 4	R^2	R^3	Inhibition rate (%)	IC_{50} (μg/ml)
4a	Me	CO_2Et	78.93 ± 2.33	12.96 ± 1.34
4b	Me	$COCH_3$	77.56 ± 4.87	14.84 ± 2.95
4c	*t*-Bu	imidazol-1-yl	68.14 ± 2.38	22.00 ± 0.61

group (CON) cannot interact with NA cavity. This may be the reason why the activity of compound **3b** is so poor.

As to the docking result of compound **2d** (Figures 5c1 and 6c2), the extension direction and hydrogen bond interaction of compound **2e** are similar to the docking result of compound **1p**. There are also eight hydrogen bonds formed between compound **2e** and the amino acid residues of NA. The 4-OH-3-OMe group on the benzene ring always forms two hydrogen bonds with residues of Arg152, Trp178. In addition, the carbonyl of the amide group (CON) of compound **2e** can interact with residues of Arg371, Try406, and Arg118 by four hydrogen bonds. The CO_2Et substituent at the 5-position on the thiazole ring also formed two hydrogen bonds with Arg292 and Asn294. As shown in the Figures 5d1 and 6d2, compared with compound **2d**, the molecular structure of compound **4a** extends more flatly without some folding in the molecule. An unfolded molecule ensures a stronger binding force to the NA cavity, which is very similar with oseltamivir. So the six hydrogen bonds on the rigid structure of compound **4a** guarantee that compound **4a** produces a stronger interaction with the NA cavity.

To sum up, the docking results of compounds **1p**, **2d**, **3b**, and **4a** demonstrate that the 4-OH-3-OMe group on the benzene ring of ferulic acid amide derivatives is dominant on NA inhibitor activity, and the amide group (CON) of ferulic acid amide derivatives has a great contribution to the improvement of activity. These two sites are just like two fulcrums to make sure that the ferulic acid derivatives can combine with the NA cavity.

3 | CONCLUSIONS

Four series of ferulic acid derivatives were designed, synthesized, and evaluated for their ability to inhibit NA of influenza H1N1 virus. Compound **2c** was confirmed by single-crystal X-ray diffraction, and the C=C double bond was further confirmed as the form of geometric *E* isomer. Biological activity results indicated that ferulic acid derivatives containing the 4-OH-3-OMe group on the benzene ring always showed much better NA inhibitory activity than ferulic acid. The most two potent compounds were **1m** and **4a** with IC_{50} values of 12.77 ± 0.47 and 12.96 ± 1.34 μg/ml, respectively. Structure–activity relationship investigation suggested that the 4-OH-3-OMe group on the benzene ring of ferulic acid derivatives was the pivotal pharmacophore. Increasing hydrophilicity and polarity of ferulic acid derivatives were beneficial to improve NA inhibitory activity. The carbon–carbon double bonds played a key role in the activity of ferulic acid piperazine amide derivatives **1**. However, carbon–carbon double bonds had almost no effect on the activity of ferulic acid thiazolylamide derivatives **2**. Molecular docking demonstrated the interaction mode of each series of the compound with the NA active cavity. Besides, it also preliminarily explained the reason why each series of compounds possesses different activities. It was found that the 4-OH-3-OMe group and amide group (CON) of ferulic acid amide derivatives were two key pharmacophores on NA inhibitory activity. Ferulic acid has the potential to be further modified to have better NA inhibitory activity.

4 | EXPERIMENTS

4.1 | Chemistry

4.1.1 | General

Starting materials and solvents were commercially available and used without further purification. All reactions were monitored by thin-layer chromatography (TLC) on 25.4- to 6.2-mm silica gel plates (GF-254). Melting points were measured on an X-4 electrothermal digital melting point apparatus and uncorrected. Nuclear magnetic resonance (NMR) was recorded on a Varian INOVA-400 spectrometer using tetramethylsilane (TMS) as an internal standard. The solvents for NMR were dimethyl sulfoxide (DMSO)-d_6.

The InChI codes of the investigated compounds together with some biological activity data are provided as Supporting Information.

4.1.2 | General procedure for the synthesis of compounds 1a–q

The substituted cinnamic acids were synthesized according to the method reported in reference[23] with substituted benzaldehydes and malonic acid as the raw materials. A mixture of

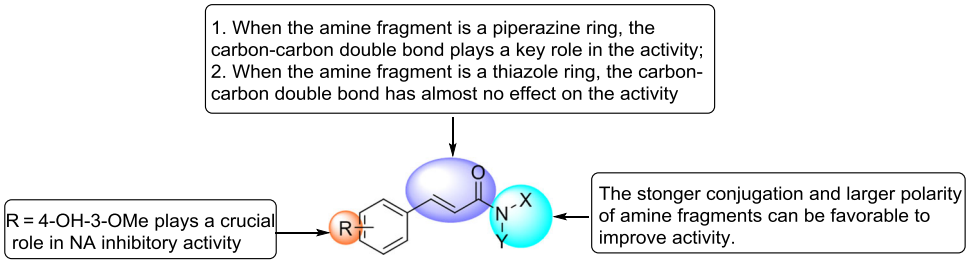

FIGURE 4 Structure–activity relationship of the ferulic acid derivatives

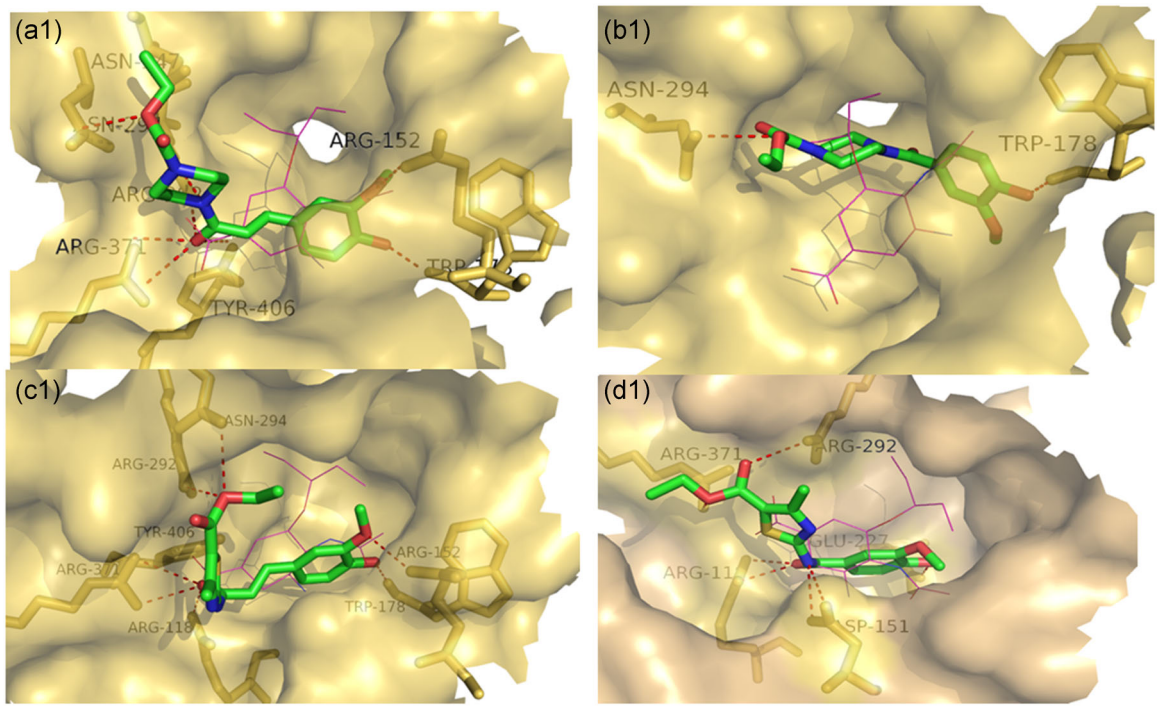

FIGURE 5 Specific interactions of compounds **1p** (a1), **3b** (b1), **2d** (c1), and **4a** (d1) binding to the active site of neuraminidase (H1N1, PDB: 3TI6)

different substituted cinnamic acids **6** (1.2 mmol), 1-hydroxybenzotriazole (1.2 mmol), *N*-(3-dimethylaminopropyl)-*N*′-ethylcarbodiimide hydrochloride (1.2 mmol) in *N*,*N*-dimethylformamide (10 ml) was stirred for 30 min, and then piperazine derivatives **7** (1 mmol) were added. The reaction mixture was kept stirring at room temperature for 8–12 hr confirmed by TLC and then poured into ice water. The mixture was extracted with ethyl acetate. Organic phase was washed successively with saturated sodium bicarbonate, dilute hydrochloric acid solution, and saturated sodium chloride solution, dried over anhydrous sodium sulfate, filtered, and evaporated. The crude product was recrystallized from ethanol to afford the pure compounds **1a–q**.

*(E)-3-(3-Hydroxyphenyl)-1-(4-(4-hydroxyphenyl)piperazin-1-yl)-prop-2-en-1-one (**1a**)*

Yellow solid. Yield 61.5%; m.p. 222–225°C; ^{1}H NMR (400 MHz, DMSO-d_6) δ: 2.99 (br, 4H, 2 × CH_2), 3.72 (br, 2H, CH_2), 3.84 (br, 2H, CH_2), 6.70 (d, J = 8.2 Hz, 2H, C_6H_4), 6.82–7.26 (m, 7H, C_6H_3, C_6H_4, CH), 7.44 (d, J = 15.4 Hz, 1H, CH), 9.00 (s, 1H, OH), and 9.67 (s, 1H, OH); ^{13}C NMR (101 MHz, DMSO-d_6) δ: 45.62, 51.49, 115.02, 115.97, 117.15, 118.43, 118.92, 119.41, 130.14, 136.89, 142.27, 144.38, 151.87, 158.14, and 164.92.

*(E)-3-(4-Hydroxyphenyl)-1-(4-(4-hydroxyphenyl)piperazin-1-yl)-prop-2-en-1-one (**1b**)*

Yellow solid. Yield 56.3%, m.p. 223–226°C; ^{1}H NMR (400 MHz, DMSO-d_6) δ: 2.98 (br, 4H, 2 × CH_2), 3.71–3.83 (m, 4H, 2 × CH_2), 6.70 (d, J = 8.0 Hz, 2H, C_6H_4), 6.82–6.86 (m, 4H, C_6H_4, C_6H_4), 7.10 (d, J = 15.2 Hz, 1H, CH), 7.46 (d, J = 15.2 Hz, 1H, CH), 7.59 (d, J = 7.6 Hz, 2H, C_6H_4), 9.00 (s, 1H, OH), and 10.01 (s, 1H, OH); ^{13}C NMR (101 MHz, DMSO-d_6) δ: 45.58, 51.48, 114.72, 115.98, 116.06, 118.89, 126.61, 130.25, 142.39, 144.38, 151.89, 159.53, and 165.30.

*(E)-3-(3,4-Dihydroxyphenyl)-1-(4-(4-hydroxyphenyl)piperazin-1-yl)-prop-2-en-1-one (**1c**)*

Light yellow solid. Yield 73.3%; m.p. 233–235°C; ^{1}H NMR (400 MHz, DMSO-d_6) δ: 3.00 (br, 4H, 2 × CH_2), 3.74–3.85 (m, 4H, 2 × CH_2), 6.71–7.16 (m, 8H, C_6H_3, C_6H_4, CH), 7.41 (d, J = 15.2 Hz, 1H, CH), 8.96 (s, 1H, OH), 9.06 (s, 1H, OH), and 9.54 (s, 1H, OH); ^{13}C NMR (101 MHz, DMSO-d_6) δ: 114.69, 115.38, 115.97, 116.06, 118.90, 121.12, 127.20, 142.75, 144.42, 145.89, 147.84, 151.82, and 165.28.

*(E)-1-(4-(4-Hydroxyphenyl)piperazin-1-yl)-3-(4-methoxyphenyl)-prop-2-en-1-one (**1d**)*

Yellow solid. Yield 61.2%; m.p. 196–198°C; ^{1}H NMR (400 MHz, DMSO-d_6) δ: 2.96 (br, 4H, 2 × CH_2), 3.70 (br, 2H, CH_2), 3.79 (s, 3H, OCH_3), 3.82 (br, 2H, CH_2), 6.68 (d, J = 8.2 Hz, 2H, C_6H_4), 6.83 (d, J = 8.2 Hz, 2H, C_6H_4), 6.97 (d, J = 8.2 Hz, 2H, C_6H_4), 7.16 (d, J = 15.3 Hz, 1H, CH), 7.49 (d, J = 15.3 Hz, 1H, CH), 7.69 (d, J = 8.2 Hz, 2H, C_6H_4), and 8.90 (s, 1H, OH); ^{13}C NMR (101 MHz, DMSO-d_6) δ: 45.57, 51.50, 55.73, 114.65, 115.93, 115.96, 118.92, 128.25, 130.16, 141.92, 144.41, 151.85, 160.88, and 165.15.

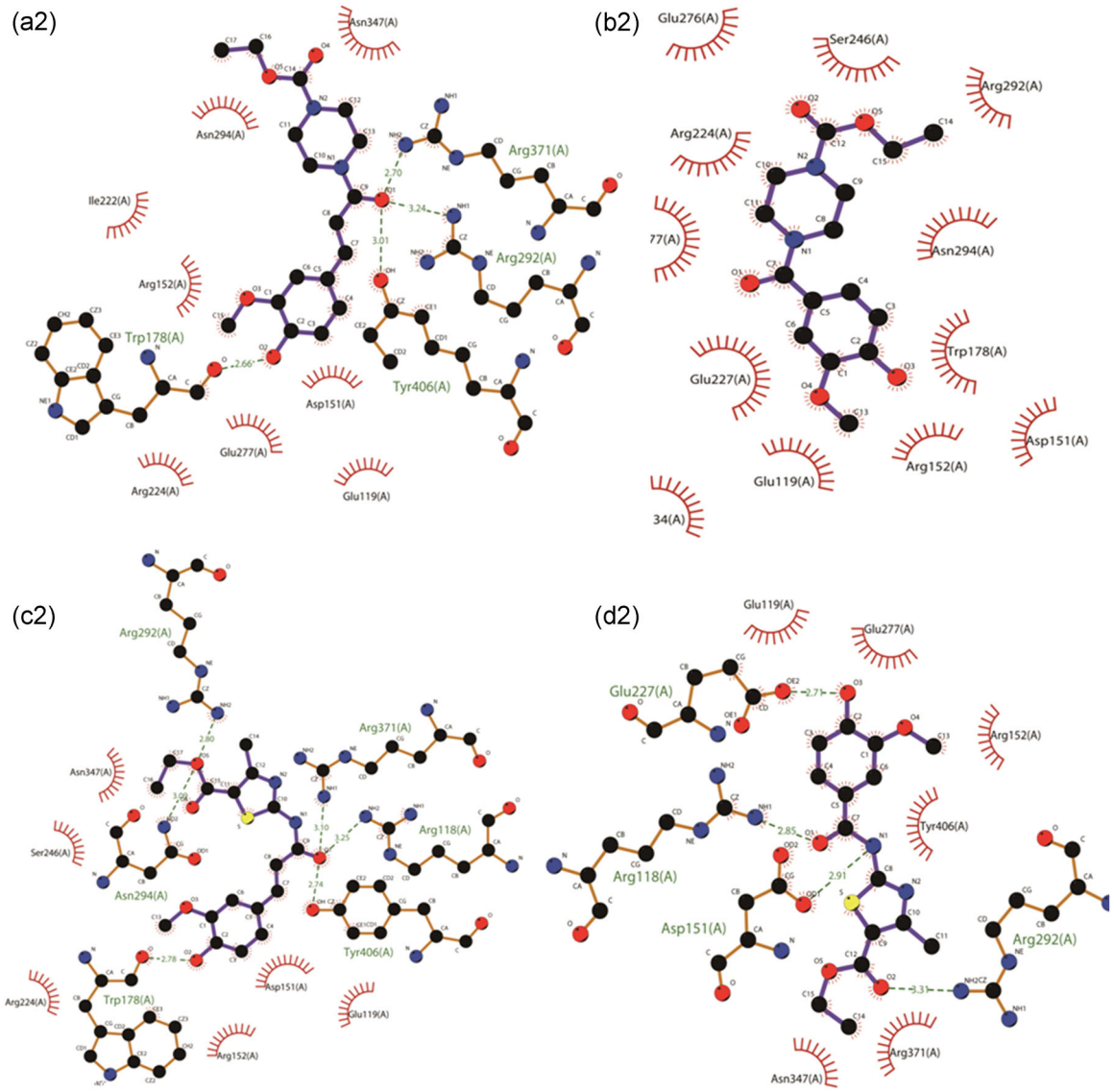

FIGURE 6 Two-dimensional binding mode of compounds **1p** (a2), **3b** (b2), **2d** (c2), and **4a** (d2) binding to the active site of neuraminidase (H1N1, PDB: 3TI6)

*(E)-1-(4-(4-Hydroxyphenyl)piperazin-1-yl)-3-(4-nitrophenyl)-prop-2-en-1-one (**1e**)*

Yellow solid. Yield 79.1%; m.p. 240–242°C; ^{1}H NMR (400 MHz, DMSO-d_6) δ: 2.99 (br, J = 5.5 Hz, 4H, 2 × CH_2), 3.72 (br, 2H, CH_2), 3.87 (br, 2H, CH_2), 6.68 (d, J = 8.0 Hz, 2H, C_6H_4), 6.84 (d, J = 8.0 Hz, 2H, C_6H_4), 7.55 (d, J = 15.4 Hz, 1H, CH), 7.62 (d, J = 15.4 Hz, 1H, CH), 8.03 (d, J = 8.0 Hz, 2H, C_6H_4), 8.25 (d, J = 8.0 Hz, 2H, C_6H_4), and 8.90 (s, 1H, OH); ^{13}C NMR (101 MHz, DMSO-d_6) δ: 45.71, 51.50, 115.97, 118.95, 123.28, 124.31, 129.54, 139.49, 142.24, 144.34, 147.98, 151.89, and 164.26.

*(E)-Methyl-4-(3-(4-(4-hydroxyphenyl)piperazin-1-yl)-3-oxoprop-1-en-1-yl)benzoate (**1f**)*

White solid. Yield 80.3%; m.p. 218–222°C; ^{1}H NMR (400 MHz, DMSO-d_6) δ: 3.00 (br, 4H, 2 × CH_2), 3.73 (br, 2H, CH_2), 3.82–3.94 (m, 5H, CH_2, OCH_3), 6.70 (d, J = 8.4 Hz, 2H, C_6H_4), 6.85 (d, J = 8.4 Hz, 2H, C_6H_4), 7.49 (d, J = 15.4 Hz, 1H, CH), 7.58 (d, J = 15.4 Hz, 1H, CH), 7.91 (d, J = 8.0 Hz, 2H, C_6H_4), 7.99 (d, J = 8.0 Hz, 2H, C_6H_4), and 9.00 (s, 1H, OH); ^{13}C NMR (101 MHz, DMSO-d_6) δ: 42.30, 45.71, 52.71, 116.01, 118.92, 121.44, 128.71, 129.97, 130.42, 140.15, 140.62, 144.28, 151.91, 164.60, and 166.35.

*(E)-3-(3-Hydroxy-4-methoxyphenyl)-1-(4-(4-hydroxyphenyl)-piperazin-1-yl)prop-2-en-1-one (**1g**)*

White solid. Yield 76.0%; m.p. 234–236°C; ^{1}H NMR (400 MHz, DMSO-d_6) δ: 2.98 (br, 4H, 2 × CH_2), 3.72 (br, 2H, CH_2), 3.78–3.92 (m, 5H, CH_2, OCH_3), 6.70 (d, J = 8.1 Hz, 2H, C_6H_4), 6.85 (d, J = 8.0 Hz, 2H, C_6H_4), 6.96 (d, J = 8.0 Hz, 1H, C_6H_3), 7.09 (d, J = 15.2, 1H, CH), 7.14 (d, J = 8.0 Hz, 1H, C_6H_3), 7.21 (s, 1H, C_6H_3), 7.42 (d, J = 15.2 Hz, 1H, CH), 8.93 (s, 1H, OH), and 9.09 (s, 1H, OH); ^{13}C NMR (101 MHz, DMSO-d_6) δ: 42.23, 45.57, 56.11, 112.34, 114.76, 115.77, 115.97, 118.91, 121.10, 128.57, 142.39, 144.41, 147.00, 149.71, 151.82, and 165.19.

*(E)-3-(4-Hydroxy-3,5-dimethoxyphenyl)-1-(4-(4-hydroxyphenyl)-piperazin-1-yl)prop-2-en-1-one (**1h**)*

Yellow solid. Yield 42.5%; m.p. 229–231°C; ^{1}H NMR (400 MHz, DMSO-d_6) δ: 3.00 (br, 4H, 2 × CH_2), 3.73 (br, 2H, CH_2), 3.80–3.92 (m, 8H, CH_2, 2 × OCH_3), 6.71 (d, J = 8.0 Hz, 2H, C_6H_4), 6.86 (d, J = 8.0 Hz, 2H, C_6H_4), 7.06 (s, 2H, C_6H_2), 7.18 (d, J = 15.2 Hz, 1H, CH), 7.48 (d, J = 15.2 Hz, 1H, CH), 8.85 (s, 1H, OH), and 8.97 (s, 1H, OH); ^{13}C NMR (101 MHz, DMSO-d_6) δ: 56.57, 106.21, 115.15, 116.04, 119.02, 125.94, 137.80, 143.36, 144.38, 148.40, 151.65, and 165.68.

*(E)-3-(4-Hydroxy-3-methoxyphenyl)-1-(4-(4-hydroxyphenyl)-piperazin-1-yl)prop-2-en-1-one (**1i**)*

Brownish yellow solid. Yield 56.9%; m.p. 225–227°C; ^{1}H NMR (400 MHz, DMSO-d_6) δ: 2.97 (br, 4H, 2 × CH_2), 3.71 (br, 4H, 2 × CH_2), 3.83 (s, 3H, OCH_3), 6.67 (d, J = 8.0 Hz, 2H, C_6H_4), 6.78 (d, J = 8.0 Hz, 1H, C6H3), 6.8 (d, J = 8.0 Hz, 2H, C_6H_4), 7.08–7.12 (m, 2H, C_6H_3, CH), 7.34 (s, 1H, C_6H_3), 7.43 (d, J = 15.2 Hz, 1H, CH), 8.89 (s, 1H, OH), and 9.42 (s, 1H, OH); ^{13}C NMR (101 MHz, DMSO-d_6) δ: 45.48, 50.93, 56.26, 111.60, 114.89, 115.90, 115.98, 118.95, 123.04, 127.15, 142.85, 148.31, 148.92, 151.84, and 165.39.

*(E)-3-(4-Hydroxy-3-methoxyphenyl)-1-(4-(2-methoxyphenyl)-piperazin-1-yl)prop-2-en-1-one (**1j**)*

White solid. Yield 65.2%; m.p. 123–125°C; ^{1}H NMR (400 MHz, DMSO-d_6) δ: 2.97 (br, 4H, 2 × CH_2), 3.72 (br, 2H CH_2), 3.80 (s, 3H, OCH_3), 3.84 (br, 5H, OCH_3, CH_2), 6.78 (d, J = 8.0 Hz, 1H, C_6H_3), 6.90 (m, 2H, C_6H_4), 6.97 (m, 2H, C_6H_4), 7.10–7.13 (m, 2H, C_6H_3, CH), 7.36 (s, 1H, C_6H_3), 7.45 (d, J = 15.1 Hz, 1H, CH), and 9.46 (s, 1H, OH); ^{13}C NMR (101 MHz, DMSO-d_6) δ: 45.76, 51.35, 55.83, 56.26, 111.56, 112.40, 114.92, 115.90, 118.79, 121.31, 123.07, 123.32, 127.18, 141.27, 142.78, 148.33, 148.95, 152.51, and 165.31.

*(E)-1-(4-(4-Chlorophenyl)piperazin-1-yl)-3-(4-hydroxy-3-methoxyphenyl)prop-2-en-1-one (**1k**)*

Brownish yellow solid. Yield 87.9%; m.p. 136–138°C; ^{1}H NMR (400 MHz, DMSO-d_6) δ: 3.19 (br, 4H, 2 × CH_2), 3.74 (br, 2H, CH_2), 3.87 (m, 5H, CH_2, OCH_3), 6.81 (d, J = 8.0 Hz, 1H, C_6H_3), 7.02 (d, J = 8.4 Hz, 2H, C_6H_4), 7.13–7.16 (m, 2H, C_6H_3 + CH), 7.28 (d, J = 8.4 Hz, 2H, C_6H_4), 7.38 (s, 1H, C_6H_3), 7.48 (d, J = 15.2 Hz, 1H, CH), and 9.50 (s, 1H, OH); ^{13}C NMR (101 MHz, DMSO-d_6) δ: 45.14, 49.27, 56.28, 111.71, 114.83, 115.91, 117.73, 123.07, 123.25, 127.14, 129.14, 142.91, 148.31, 148.98, 150.09, and 165.3.

*(E)-3-(4-Hydroxy-3-methoxyphenyl)-1-(4-phenylpiperazin-1-yl)-prop-2-en-1-one (**1l**)*

Yellow solid. Yield 95.0%; m.p. 158–160°C; ^{1}H NMR (400 MHz, DMSO-d_6) δ: 3.19 (br, 4H, 2 × CH_2), 3.75 (br, 2H, CH_2), 3.87 (s + br, 5H, CH_2, OCH_3), 6.81–7.28 (m, 8H, C_6H_5, C_6H_3, CH), 7.39 (s, 1H, C_6H_3), 7.48 (d, J = 15.2 Hz, 1H, CH), and 9.50 (s, 1H, OH); ^{13}C NMR (101 MHz, DMSO-d_6) δ: 45.28, 49.53, 56.28, 111.68, 114.88, 115.91, 116.34, 119.78, 123.07, 127.16, 129.45, 142.87, 148.32, 148.97, 151.31, and 165.37.

*(E)-3-(4-Hydroxy-3-methoxyphenyl)-1-(4-methylpiperazin-1-yl)-prop-2-en-1-one (**1m**)*

Yellow solid. Yield 72.5%; m.p. 65–66°C; ^{1}H NMR (400 MHz, DMSO-d_6) δ: 2.22 (s, 3H, NCH_3), 2.34 (br, 4H, 2 × CH_2), 3.58–3.71 (m, 4H, 2 × CH_2), 3.86 (s, 3H, OCH_3), 6.80 (d, J = 8.0 Hz, 1H, C_6H_3), 7.06–7.12 (m, 2H, C_6H_3, CH), 7.35 (s, 1H, C_6H_3), 7.43 (d, J = 15.2 Hz, 1H, CH), and 9.46 (s, 1H, OH).

*(E)-1-(4-Ethylpiperazin-1-yl)-3-(4-hydroxy-3-methoxyphenyl)-prop-2-en-1-one (**1n**)*

Yellow solid. Yield 66.2%; m.p. 55–58°C; ^{1}H NMR (400 MHz, DMSO-d_6) δ: 1.04 (t, J = 7.2 Hz, 3H, CH_3), 2.37–2.38 (m, 6H, 2 × CH_2, NCH_2), 3.58 (br, 4H, 2 × CH_2), 3.72 (br, 4H, 2 × CH_2), 3.84 (s, 3H, OCH_3), 6.83 (d, J = 8.0 Hz, 1H, C_6H_3), 7.06–7.11 (m, 2H, C_6H_3, CH), 7.34 (s, 1H, C_6H_3), 7.42 (d, J = 15.2 Hz, 1H, CH), and 9.68 (s, 1H, OH).

*(E)-1-(4-Acetylpiperazin-1-yl)-3-(4-hydroxy-3-methoxyphenyl)-prop-2-en-1-one (**1o**)*

White solid. Yield 58.9%; m.p. 168–171°C; ^{1}H NMR (400 MHz, DMSO-d_6) δ: 2.04 (s, 3H, $COCH_3$), 3.48 (br, 4H, 2 × CH_2), 3.67 (br, 4H, 2 × CH_2), 3.83 (s, 3H, OCH_3), 6.78 (d, J = 7.9 Hz, 1H, C_6H_3), 7.05–7.12 (m, 2H, C_6H_3, CH), 7.33 (s, 1H, C_6H_3), 7.44 (d, J = 15.2 Hz, 1H, CH), and 9.47 (s, 1H, OH); ^{13}C NMR (101 MHz, DMSO-d_6) δ: 21.72, 56.26, 111.69, 114.80, 115.90, 123.04, 127.08, 142.99, 148.29, 149.00, 165.52, and 168.95.

*(E)-Ethyl-4-(3-(4-hydroxy-3-methoxyphenyl)acryloyl)-piperazine-1-carboxylate (**1p**)*

White solid. Yield 96.7%, m.p. 140–142°C; ^{1}H NMR (400 MHz, DMSO-d_6) δ: 1.20 (t, J = 6.7 Hz, 3H, CH_3), 3.41 (br, 4H, 2 × CH_2), 3.57 (br, 2H, CH_2), 3.71 (br, 2H, CH_2), 3.83 (s, 3H, OCH_3), 4.07 (q, J = 6.8 Hz, 2H, OCH_2), 6.78 (d, J = 8.0 Hz, 1H, C_6H_3), 7.03–7.11 (m, 2H, C_6H_3, CH), 7.33 (s, 1H, C_6H_3), 7.44 (d, J = 15.2 Hz, 1H, CH), and 9.46 (s, 1H, OH); ^{13}C NMR (101 MHz, DMSO-d_6) δ: 15.01, 56.26, 61.43, 111.68, 114.76, 115.92, 123.03, 127.09, 143.06, 148.32, 149.00, 155.13, and 165.57.

*(E)-tert-Butyl-4-(3-(4-hydroxy-3-methoxyphenyl)acryloyl)-piperazine-1-carboxylate (**1q**)*

White solid. Yield 94.3%, m.p. 191–193°C; ^{1}H NMR (400 MHz, $CDCl_3$) δ: 1.48 (s, 9H, 3 × CH_3), 3.49 (br, 4H, 2 × CH_2), 3.67 (br, 4H, 2 × CH_2), 3.93 (s, 3H, OCH_3), 6.70 (d, J = 15.2 Hz, 1H, COCH), 6.92 (d, J = 8.2 Hz, 1H, C_6H_3), 6.99 (s, 1H, C_6H_3), 7.09 (d, J = 8.2 Hz, 1H, C_6H_3), and 7.63 (d, J = 15.2 Hz, 1H, CH). ^{13}C NMR (101 MHz, $CDCl_3$-d_6) δ: 28.39, 56.01, 80.38, 109.95, 113.97, 114.84, 122.07, 127.60, 143.61, 146.82, 147.62, 154.62, and 166.01.

4.1.3 | Synthesis of (*E*)-3-(4-hydroxy-3-methoxyphenyl)-1-(piperazin-1-yl)prop-2-en-1-one hydrochloride (1r)

A solution of compound **1q** (1 mmol) in dry ethyl acetate (10 ml) was passed into dry hydrogen chloride gas at room temperature and

stirred for 2 hr confirmed by TLC. Then the precipitate was filtered and washed with ethyl acetate to afford the pure compound **1r**. White solid. Yield 95.9%; m.p. 196–198°C; ^{1}H NMR (400 MHz, DMSO-d_6) δ: 3.12 (br, 4H, 2 × CH_2), 3.83 (s, 3H, OCH_3), 3.95 (br, 3H, 2 × CH_2), 6.82 (d, J = 7.6 Hz, 1H, C_6H_3), 7.06–7.13 (m, 2H, C_6H_3, CH), 7.34 (s, 1H, C_6H_3), 7.48 (d, J = 15.2 Hz, 1H, CH), 9.56 (s, 1H, OH), and 9.60 (s, 2H, NH_2); ^{13}C NMR (101 MHz, $CDCl_3$-d_6) δ: 43.25, 56.33, 111.85, 114.27, 115.96, 123.18, 126.94, 143.59, 148.33, 149.22, and 165.66.

4.1.4 | Synthesis of (*E*)-4-(3-(4-(4-hydroxyphenyl)-piperazin-1-yl)-3-oxoprop-1-en-1-yl)benzoic acid (1s)

To a solution of compound **1p** (1 mmol) in ethanol (10 ml) was added 2 N lithium hydroxide solution (2 ml) and stirred for 8 hr confirmed by TLC. Then, dilute hydrochloric acid was added into the reaction solution to adjust pH to 4–5. The precipitate was filtered and washed with water to afford the pure product **1s**. White solid. Yield 70.0%; m.p. 285–288°C; ^{1}H NMR (400 MHz, DMSO-d_6) δ: 2.98 (br, 4H, 2 × CH_2), 3.72 (br, 2H, CH_2), 3.86 (br, 2H, CH_2), 6.68 (d, J = 8.3 Hz, 2H, C_6H_4), 6.84 (d, J = 8.3 Hz, 2H, C_6H_4), 7.45 (d, J = 15.4 Hz, 1H, CH), 7.57 (d, J = 15.4 Hz, 1H, CH), 7.86 (d, J = 7.9 Hz, 2H, C_6H_4), 7.96 (d, J = 7.9 Hz, 2H, C_6H_4), 8.94 (s, 1H, OH), and 13.00 (s, 1H, COOH); ^{13}C NMR (101 MHz, DMSO-d_6) δ: 45.59, 51.71, 116.01, 119.14, 121.10, 128.56, 130.10, 131.69, 139.79, 140.81, 164.57, and 167.36.

4.1.5 | General procedure for the synthesis of compounds 2a–f

A mixture of ferulic acid derivative **3** (1.2 mmol), 1-hydroxybenzotriazole (1.2 mmol), *N*-(3-dimethylaminopropyl)-*N*′-ethylcarbodiimide hydrochloride (1.2 mmol) in *N*,*N*-dimethylformamide (10 ml) was stirred for 30 min and then 2-aminothiazolyl derivative **4** (1 mmol) was added. The mixture was stirred at 115°C for 8–16 hr confirmed by TLC, and cooled at room temperature. The reaction solution was poured into ice water. The precipitate was filtered and washed successively with saturated sodium bicarbonate, dilute hydrochloric acid solution, and water, recrystallized from ethanol to afford the pure product **2a–f**.

*(E)-N-(4-(tert-Butyl)-5-nitrothiazol-2-yl)-3-(4-hydroxy-3-methoxyphenyl)acrylamide (**2a**)*

Red solid. Yield 36.8%, m.p. 262–263°C; ^{1}H NMR (400 MHz, DMSO-d_6) δ: 1.50 (s, 9H, 3 × CH_3), 3.88 (s, 3H, CH_3), 6.82 (d, J = 15.6 Hz, 1H, CH), 6.91 (d, J = 8.0 Hz, 1H, C_6H_3), 7.19 (d, J = 8.0 Hz, 1H, C_6H_3), 7.26 (s, 1H, C_6H_3), 7.79 (d, J = 15.6 Hz, 1H, CH), 9.81 (s, 1H, OH), and 13.01 (s, 1H, NH); ^{13}C NMR (101 MHz, DMSO-d_6) δ: 28.48, 36.95, 56.03, 112.28, 115.09, 116.36, 123.13, 125.94, 137.86, 145.55, 148.37, 150.31, 158.34, 163.32, and 165.55.

*(E)-N-(4-(tert-Butyl)-5-(1H-imidazol-1-yl)thiazol-2-yl)-3-(4-hydroxy-3-methoxyphenyl)acrylamide (**2b**)*

Light yellow solid. Yield 38.2%, m.p. 244–246°C; ^{1}H NMR (400 MHz, DMSO-d_6) δ: 1.15 (s, 9H, 3 × CH_3), 3.85 (s, 3H, OCH_3), 6.77 (d, J = 15.6 Hz, 1H, CH), 6.88 (d, J = 7.6 Hz, 1H, C_6H_3), 7.12–7.14 (m, 2H, $N_2C_3H_3$, C_6H_3), 7.21 (s, 1H, C_6H_3), 7.47 (s, 1H, $N_2C_3H_3$), 7.67 (d, J = 15.6 Hz, 1H, CH), 7.94 (s, 1H, $N_2C_3H_3$), 9.71 (s, 1H, OH), and 12.40 (s, 1H, NH); ^{13}C NMR (101 MHz, DMSO-d_6) δ: 29.89, 35.76, 56.04, 112.18, 116.01, 116.34, 119.71, 122.62, 124.70, 126.17, 129.19, 143.91, 148.34, 149.86, 153.73, 153.89, and 164.57.

*(E)-N-(4-(tert-Butyl)-5-(1H-1,2,4-triazol-1-yl)thiazol-2-yl)-3-(4-hydroxy-3-methoxyphenyl)acrylamide (**2c**)*

Light yellow solid. Yield 40.1%, m.p. 126–128°C; ^{1}H NMR (400 MHz, DMSO-d_6) δ: 1.14 (s, 9H, 3 × CH_3), 3.85 (s, 3H, OCH_3), 6.78 (d, J = 15.6 Hz, 1H, CH), 6.88 (d, J = 8.0 Hz, 1H, C_6H_3), 7.14 (d, J = 8.0 Hz, 1H, C_6H_3), 7.22 (s, 1H, C_6H_3), 7.69 (d, J = 15.6 Hz, 1H, CH), 8.28 (s, 1H, $N_3C_2H_2$), 8.98 (s, 1H, $N_3C_2H_2$), 9.74 (s, 1H, OH), and 12.53 (s, 1H, NH); ^{13}C NMR (101 MHz, DMSO-d_6) δ: 29.74, 35.83, 56.05, 112.23, 115.91, 116.35, 119.03, 122.66, 126.15, 144.09, 148.33, 149.11, 149.90, 152.70, 154.73, 155.34, and 164.70.

*(E)-Ethyl-2-(3-(4-hydroxy-3-methoxyphenyl)acrylamido)-4-methylthiazolyl-5-carboxylate (**2d**)*

Light yellow solid. Yield 40.2%, m.p. 185–187°C; ^{1}H NMR (400 MHz, DMSO-d_6) δ: 1.29 (t, J = 7.0 Hz, 3H, CH_3), 2.56 (s, 3H, CH_3), 3.83 (s, 3H, OCH_3), 4.25 (q, J = 7.0 Hz, 2H, OCH_2), 6.71 (d, J = 15.6 Hz, 1H, CH), 6.85 (d, J = 8.0 Hz, 1H, C_6H_3), 7.12 (d, J = 8.0 Hz, 1H, C_6H_3), 7.21 (s, 1H, C_6H_3), 7.67 (d, J = 15.6 Hz, 1H, CH), 9.70 (s, 1H, OH), and 12.54 (s, 1H, NH); ^{13}C NMR (101 MHz, DMSO-d_6) δ: 14.60, 17.48, 56.06, 61.23, 112.00, 115.86, 116.32, 116.67, 123.77, 125.92, 129.18, 148.44, 150.65, 153.49, 162.87, 167.69, and 191.54.

*(E)-N-(5-Acetyl-4-methylthiazol-2-yl)-3-(4-hydroxy-3-methoxyphenyl)acrylamide (**2e**)*

Yellow solid. Yield 34.6%, m.p. 256–258°C; ^{1}H NMR (400 MHz, DMSO-d_6) δ: 2.43 (s, 3H, CH_3), 2.45 (s, 3H, CH_3), 3.77 (s, 3H, OCH_3), 6.66 (d, J = 16.0 Hz, 1H, CH), 6.80 (d, J = 8.0 Hz, 1H, C_6H_3), 7.06 (d, J = 8.0 Hz, 1H, C_6H_3), 7.15 (s, 1H, C_6H_3), 7.61 (d, J = 16.0 Hz, 1H, CH), 9.69 (s, 1H, OH), and 12.49 (s, 1H, NH); ^{13}C NMR (101 MHz, DMSO-d_6) δ: 18.59, 30.50, 56.07, 112.04, 115.90, 116.28, 122.95, 126.02, 126.09, 144.39, 148.34, 149.95, and 154.99.

*(E)-Ethyl-2-(2-(3-(4-Hydroxy-3-methoxyphenyl)acrylamido)-thiazol-4-yl)acetate (**2f**)*

Light yellow solid. Yield 32.1%, m.p. 181–183°C; ^{1}H NMR (400 MHz, DMSO-d_6) δ: 1.19 (t, J = 7.0 Hz, 3H, CH_3), 3.70 (s, 2H, CH_2), 3.83 (s, 3H, OCH_3), 4.09 (q, J = 7.1 Hz, 2H, OCH_2), 6.69 (d, J = 15.6 Hz, 1H, CH), 6.85 (d, J = 8.0 Hz, 1H, C_6H_3), 6.99 (s, 1H, SNC_3H), 7.09 (d, J = 8.0 Hz, 1H, C_6H_3), 7.18 (s, 1H, C_6H_3), 7.62 (d, J = 15.6 Hz, 1H, CH), 9.64 (s, 1H, OH), and 12.24 (s, 1H, NH); ^{13}C NMR (101 MHz, DMSO-d_6) δ: 14.57, 37.19, 56.07, 60.79, 111.03, 112.05, 116.32,

116.56, 122.59, 126.29, 143.30, 144.31, 148.35, 149.71, 158.36, 164.11, and 170.53.

4.1.6 | Synthesis of (2*E*)-3-(4-hydroxy-3-methoxyphenyl)-*N*-(5-(1-(methoxyimino)-ethyl)-4-methylthiazol-2-yl)acrylamide (2g)

To a solution of compound **2e** (0.5 mmol) in *N*,*N*-dimethylformamide (5 ml) was added the mixed aqueous solution (2 ml) of methoxyammonium chloride (1 mmol) and sodium acetate (1 mmol). Then the mixture was stirred at 80°C for 10 hr confirmed by TLC and cooled at room temperature. The reaction solution was poured into ice water. The precipitate was filtered and washed successively with saturated sodium bicarbonate and water to afford the pure product **2g**. White solid. Yield 60.6%, m.p. 133–135°C; ^{1}H NMR (400 MHz, DMSO-d_6) δ: 2.23 (s, 2H, C_3NSCH_3, *E*-type), 2.43 (s, 1H, C_3NSCH_3, *Z*-type), 2.26 (s, 1H, CH_3, *Z*-type), 2.45 (s, 2H, CH_3, *E*-type), 3.85 (s, 3H, OCH_3), 3.90 (s, 3H, $NOCH_3$), 6.72 (d, J = 15.6 Hz, 1H, CH), 6.87 (d, J = 8.0 Hz, 1H, C_6H_3), 7.13 (d, J = 8.0 Hz, 1H, C_6H_3), 7.22 (s, 1H, C_6H_3), 7.65 (d, J = 15.6 Hz, 1H, CH), 9.70 (s, 1H, OH), and 12.24 (s, 1H, NH).

4.1.7 | Synthesis of (*E*)-2-(2-(3-(4-hydroxy-3-methoxyphenyl)acrylamido)-thiazol-4-yl)acetic acid (2h)

To a solution of compound **2f** (1 mmol) in ethanol (10 ml) was added 2 N lithium hydroxide solution (2 ml) and stirred for 8 hr confirmed by TLC. Then dilute hydrochloric acid was added into the reaction solution to adjust pH to 4–5. The precipitate was filtered and washed with water to afford the pure product **2h**. White solid. Yield 65.9%, m.p. 210–212°C; ^{1}H NMR (400 MHz, DMSO-d_6) δ: 3.62 (s, 2H, CH_2), 3.83 (s, 3H, OCH_3), 6.69 (d, J = 15.6 Hz, 1H, CH), 6.85 (d, J = 8.0 Hz, 1H, C_6H_3), 6.96 (s, 1H, SNC_3H), 7.10 (d, J = 8.0 Hz, 1H, C_6H_3), 7.19 (s, 1H, C_6H_3), 7.63 (d, J = 15.6 Hz, 1H, CH), 9.63 (s, 1H, OH), 12.24 (s, 1H, NH), and 12.33 (s, 1H, COOH); ^{13}C NMR (101 MHz, DMSO-d_6) δ: 37.38, 56.07, 110.76, 112.02, 116.30, 116.58, 122.58, 126.28, 143.23, 144.88, 148.33, 149.67, 158.15, 164.06, and 172.05.

4.1.8 | General procedure for the synthesis of compounds 3a–c)

The same method as for the synthesis of compounds **1a–o** was carried out with vanillic acid and piperazine derivatives as raw materials and dichloromethane as the solvent to afford the products **3a–c**.

*(4-Hydroxy-3-methoxyphenyl)(4-(4-hydroxyphenyl)piperazin-1-yl)-methanone (**3a**)*

Light yellow solid. Yield 53.6%, m.p. 148–150°C; ^{1}H NMR (400 MHz, DMSO-d_6) δ: 2.98 (br, 4H, 2 × CH_2), 3.64 (br, 4H, 2 × CH_2), 3.81 (s, 3H, OCH_3), 6.69 (d, J = 8.0 Hz, 2H, C_6H_4), 6.83–6.85 (m, 3H, C_6H_3 + C_6H_4), 6.90 (d, J = 7.2 Hz, 1H, C_6H_3), 7.01 (s, 1H, C_6H_3), 8.93 (s, 1H, OH), and 9.48 (s, 1H, OH); ^{13}C NMR (101 MHz, DMSO-d_6) δ: 50.95, 56.13, 112.19, 115.36, 115.94, 118.93, 120.92, 126.87, 144.40, 147.74, 148.50, 151.82, and 169.62.

*Ethyl 4-(4-hydroxy-3-methoxybenzoyl)piperazine-1-carboxylate (**3b**)*

White solid. Yield 88.7%, m.p. 137–139°C; ^{1}H NMR (400 MHz, DMSO-d_6) δ: 1.21 (t, J = 7.0 Hz, 3H, CH_3), 3.44 (br, 4H, 2 × CH_2), 3.51 (br, 4H, 2 × CH_2), 3.81 (s, 3H, OCH_3), 4.08 (q, J = 7.0 Hz, 2H, OCH_2), 6.83 (d, J = 8.0 Hz, 1H, C_6H_3), 6.89 (d, J = 8.0, 1H, C_6H_3), 6.99 (s, 1H, C_6H_3), and 9.49 (s, 1H, OH); ^{13}C NMR (101 MHz, DMSO-d_6) δ: 15.02, 43.77, 56.12, 61.37, 112.22, 115.38, 120.99, 126.62, 147.72, 148.61, 155.08, and 169.87.

*tert-Butyl 4-(4-hydroxy-3-methoxybenzoyl)-piperazine-1-carboxylate (**3c**)*

White solid. Yield 64.3%, m.p. 56–58°C; ^{1}H NMR (400 MHz, DMSO-d_6) δ: 1.41 (s, 9H, 3 × CH_3), 3.36 (br, 4H, 2 × CH_2), 3.43 (br, 4H, 2 × CH_2), 3.79 (s, 3H, OCH_3), 6.80 (d, J = 8.0 Hz, 1H, C_6H_3), 6.86 (d, J = 8.0 Hz, 1H, C_6H_3), 6.96 (s, 1H, C_6H_3), and 9.44 (s, 1H, OH); ^{13}C NMR (101 MHz, DMSO-d_6) δ: 28.49, 44.14, 56.11, 79.63, 112.18, 115.37, 120.98, 126.66, 147.70, 148.57, 154.30, and 169.86.

4.1.9 | General procedure for the synthesis of compounds 4a–c

Acetyl vanillic acid is synthesized according to the method reported in reference.[24] White solid. Yield 76.1%, m.p. 135–136°C. Compounds **10a–c** were synthesized by the same method as for the synthesis of compound **2**. Compounds **10a–c** were hydrolyzed by the same method as for the synthesis of compound **2h** to produce the target compounds **4a–c**.

*Ethyl 2-(4-hydroxy-3-methoxybenzamido)-4-methylthiazolyl-5-carboxylate (**4a**)*

White solid. Yield 95.0%, m.p. 238–241°C; ^{1}H NMR (400 MHz, DMSO-d_6) δ: 1.32 (t, J = 7.2 Hz, 3H, CH_3), 2.61 (s, 3H, CH_3), 3.89 (s, 3H, OCH_3), 4.28 (q, J = 7.1 Hz, 2H, CH_2), 6.93 (d, J = 8.4 Hz, 1H, C_6H_3), 7.67 (d, J = 8.4, 2.0 Hz, 1H, C_6H_3), 7.77 (s, 1H, C_6H_3), 10.07 (s, 1H, OH), and 12.79 (s, 1H, NH); ^{13}C NMR (101 MHz, DMSO-d_6) δ: 14.68, 17.43, 56.22, 60.93, 112.28, 114.51, 115.72, 122.43, 123.12, 147.81, 151.81, 156.51, 161.11, 162.70, and 165.44.

*N-(5-Acetyl-4-methylthiazol-2-yl)-4-hydroxy-3-methoxybenzamide (**4b**)*

Brownish yellow solid. Yield 84.6%, m.p. 230–232°C; ^{1}H NMR (400 MHz, DMSO-d_6) δ: 2.47 (s, 3H, CH_3), 2.59 (s, 3H, CH_3), 3.86 (s, 3H, OCH_3), 6.89 (d, J = 8.4 Hz, 1H, C_6H_3), 7.64 (d, J = 8.4 Hz, 1H, C_6H_3), and 7.75 (s, 1H, C_6H_3); ^{13}C NMR (101 MHz, DMSO-d_6) δ: 18.58, 30.55, 56.17, 112.33, 115.62, 123.02, 123.57, 125.03, 151.51, 154.97, 162.45, 166.21, and 190.90.

*N-(4-(tert-Butyl)-5-(1H-imidazol-1-yl)thiazol-2-yl)-4-hydroxy-3-methoxybenzamide (**4c**)*

White solid. Yield 88.9%, m.p. 165–167°C; ^{1}H NMR (400 MHz, DMSO-d_6) δ: 1.18 (s, 9H, 3 × CH_3), 3.90 (s, 3H, OCH_3), 6.93 (d, J = 8.2 Hz, 1H, C_6H_3), 7.09 (s, 1H, $N_2C_3H_3$), 7.47 (s, 1H, $N_2C_3H_3$), 7.67 (dd, J = 8.2, 1.8 Hz, 1H, C_6H_3), 7.78 (d, J = 1.8 Hz, 1H, C_6H_3), 7.94 (s, 1H, $N_2C_3H_3$), 10.10 (s, 1H, OH), and 12.53 (s, 1H, NH); ^{13}C NMR (101 MHz, DMSO-d_6) δ: 29.87, 35.79, 56.27, 112.33, 115.63, 119.64, 122.55, 123.07, 124.69, 129.23, 141.34, 147.76, 151.68, 153.75, 154.53, and 165.38.

4.2 | NA inhibition assay

The biological test method is according to the methods reported in the literature.[25] All the target compounds were tested for their NA inhibitory activity in vitro using oseltamivir as positive control. Influenza virus A/PR/8/34, donated by the Chinese Centers for Disease Control, was used as a source of NA in enzyme inhibition assays based on the method reported by Zhang et al.[26,27] The NA was obtained by the method described by Laver et al.[28] The compound 2′-(4-methylumbellifer-yl)-α-D-acetyl neuraminic acid (MUNANA) was purchased from Sigma-Aldrich as the substrate of NA; and cleavage of this substrate by NA produces a fluorescent product, which can emit an emission wavelength of 450 nm with an excitation wavelength of 360 nm.[29] The intensity of fluorescence can reflect the activity of NA sensitively.[30]

The reaction mixture consisting of a 10 μl solution of target compounds and 30 μl NA enzyme in 33 mmol/l MES buffer (2-(*N*-morpholino)ethanesulfonic acid; pH 6.5) was added to a 96-well microtiter plate. Meanwhile, blank, enzyme, and positive drug oseltamivir were set. The reaction was started by the addition of the substrate containing 10 μl of 4 mmol/l $CaCl_2$, 20 μl of 20 μg·mmol^{-1}·l^{-1} MUNANA and 30 μl water to the plate. After incubation for 60 min, the reaction was terminated by adding 150 μl 14 mmol/l NaOH in 83% ethanol. The resulting fluorescence was quantified at an excitation wavelength of 360 nm and an emission wavelength of 450 nm. The data are expressed as the mean of three independent experiments. The IC_{50} was calculated by plotting the percent of inhibition of NA activity versus the inhibitor concentration.

4.3 | Docking study

The crystal structure data of H1N1 NA–oseltamivir complex (PDB code: 3TI6) was downloaded from the RSCB Protein Data Bank. The docked compounds **1p**, **2d**, **3b**, and **4a** were energy-minimized using the MM2 force-field. Then, LeDock was used to have the docking with default parameters.[20,21] The dimension of the binding box was set as (X_{min} = −37.4, X_{max} = −19.8, Y_{min} = 7.0, Y_{max} = 21.5, Z_{min} = 12.0, Z_{max} = 30.2). The results were analyzed and visualized by PyMOL. LigPlot + v1.4.5 was used to depict the 2D interaction diagrams.[22]

ACKNOWLEDGMENTS

This study was financially supported by the Hunan Provincial Natural Science Foundation of China (No. 2019JJ40030). The Institute of the Chinese Academy of Medical Sciences and Peking Union Medical College provided the biological activity assays.

CONFLICT OF INTEREST

The authors declare no conflict of interest.

ORCID

Ai-Xi Hu http://orcid.org/0000-0001-8676-6020

REFERENCES

[1] F. Krammer, P. Palese, *Nat. Rev. Drug Discov.* **2015**, *14*, 167.
[2] F. S. Dawood, A. D. Iuliano, C. Reed, M. I. Meltzer, D. K. Shay, P. Y. Cheng, D. Bandaranayake, R. F. Breiman, W. A. Brooks, P. Buchy, D. R. Feikin, K. B. Fowler, A. Gordon, N. T. Hien, P. Horby, Q. S. Huang, M. A. Katz, A. Krishnan, R. Lal, J. M. Montgomery, K. Mølbak, R. Pebody, A. M. Presanis, H. Razuri, A. Steens, Y. O. Tinoco, J. Wallinga, H. Yu, S. Vong, J. Bresee, M. A. Widdowson, *Lancet Infect. Dis.* **2012**, *12*, 687.
[3] P. M. Colman, J. N. Varghese, W. G. Laver, *Nature* **1983**, *303*, 41.
[4] L. M. G. Chavas, R. Kato, N. Suzuki, M. Itzstein, M. C. Mann, R. J. Thomson, J. C. Dyason, J. McKimm-Breschkin, P. Fusi, C. Tringali, B. Venerando, G. Tettamanti, E. Monti, S. Wakatsuki, *J. Med. Chem.* **2010**, *53*, 2998.
[5] E. Feng, D. Ye, J. Li, D. Zhang, J. Wang, F. Zhao, R. Hilgenfeld, M. Zheng, H. Jiang, H. Liu, *ChemMedChem* **2012**, *7*, 1527.
[6] Z. Lou, Y. Sun, Z. Rao, *Trends Pharmacol. Sci.* **2014**, *35*, 86.
[7] Y. Wu, F. Gao, J. Qi, Y. Bi, L. Fu, S. Mohan, Y. Chen, X. Li, B. M. Pinto, C. J. Vavricka, P. Tien, G. F. Gao, *J. Virol.* **2016**, *90*, 10693.
[8] M. Okomo-Adhiambo, K. Sleeman, K. Ballenger, H. T. Nguyen, V. P. Mishin, T. G. Sheu, J. Smagala, Y. Li, A. I. Klimov, L. V. Gubareva, *Viruses* **2010**, *2*, 2269.
[9] T. G. Sheu, V. M. Deyde, M. Okomo-Adhiambo, R. J. Garten, X. Xu, R. A. Bright, E. N. Butler, T. R. Wallis, A. I. Klimov, L. V. Gubareva, *Antimicrob. Agents Chemother.* **2008**, *52*, 3284.
[10] T. T. Dao, P. H. Nguyen, H. S. Lee, E. Kim, J. Park, S. I. Lim, W. K. Oh, *Bioorg. Med. Chem. Lett.* **2011**, *21*, 294.
[11] A. L. Liu, F. Yang, M. Zhu, D. Zhou, M. Lin, S. M. Lee, Y. T. Wang, G. H. Du, *Planta Med.* **2010**, *76*, 1874.
[12] A. L. Liu, H. D. Wang, S. M. Lee, Y. T. Wang, G. H. Du, *Bioorg. Med. Chem.* **2008**, *16*, 7141.
[13] H. R. El-Seedi, A. M. El-Said, S. A. Khalifa, U. Göransson, L. Bohlin, A. K. Borg-Karlson, R. Verpoorte, *J. Agri. Food Chem.* **2012**, *60*, 10877.
[14] M. Hariono, N. Abdullah, K. V. Damodaran, E. E. Kamarulzaman, N. Mohamed, S. S. Hassan, S. Shamsuddin, H. A. Wahab, *Sci. Rep.* **2016**, *6*, 38692.
[15] G. Enkhtaivan, P. Muthuraman, D. H. Kim, B. Mistry, *Bioorg. Med. Chem.* **2017**, *25*, 5185.
[16] A. X. Hu, M. Y. Cui, S. S. Li, A. L. Liu, H. Jia, *CN 107235927 B* **2019**.
[17] K. Yuan, M. Xiao, Y. Tan, J. Ye, Y. L. Xie, X. X. Sun, A. X. Hu, W. W. Lian, A. L. Liu, *Mol. Divers.* **2017**, *21*, 565.
[18] A. X. Hu, M. W. Xiao, J. Ye, X. W. Yan, W. W. Lian, A. L. Liu, *CN 106317049 B* **2018**.

[19] X. Li, J. Sheng, G. Huang, R. Ma, F. Yin, D. Song, C. Zhao, S. Ma, *Eur. J. Med. Chem.* **2015**, *97*, 32.
[20] Z. Wang, H. Sun, X. Yao, D. Li, L. Xu, S. Tian, T. Hou, *Phys. Chem. Chem. Phys.* **2016**, *18*, 12964.
[21] H. Zhao, D. Huang, A. Caflisch, *ChemMedChem* **2012**, *7*, 1983.
[22] R. A. Laskowski, M. B. Swindells, *J. Chem. Inf. Model.* **2011**, *51*, 2778.
[23] X. Li, J. Sheng, G. Huang, R. Ma, F. Yin, D. Song, C. Zhao, S Ma, *Eur. J. Med. Chem.* **2015**, *97*, 32.
[24] R. Victor, *J. Labelled Compd. Radiopharm.* **1976**, *2*, 313.
[25] M. Y. Cui, J. X. Nie, Z. Z. Yan, M. W. Xiao, D. Ling, J. Ye, A. X. Hu, *Med. Chem. Res.* **2019**, *28*, 938.
[26] T. Liu, L. Lin, H. Zhao, *Sci. China, Ser. B. Chem.* **2005**, *48*, 1.
[27] J. Zhang, Q. Wang, H. Fang, W. Xu, A. Liu, G. Du, *Bioorg. Med. Chem.* **2008**, *16*, 3839.
[28] W. G. Laver, P. M. Colman, R. G. Webster, V. S. Hinshaw, G. M. Air, *Virology* **1984**, *137*, 314.
[29] N. T. Wetherall, T. Trivedi, J. Zeller, C. Hodges-Savola, J. L. McKimm-Breschkin, M. Zambon, F. Hayden, *J. Clin. Microbiol.* **2003**, *41*, 742.
[30] P. M. Mitrasinovic, *Biophys. Chem.* **2009**, *140*, 35.

SUPPORTING INFORMATION

Additional supporting information may be found online in the Supporting Information section.

How to cite this article: Cui M-Y, Xiao M-W, Xu L-J, et al. Bioassay of ferulic acid derivatives as influenza neuraminidase inhibitors. *Arch Pharm Chem Life Sci*. 2019;e1900174. https://doi.org/10.1002/ardp.201900174